Superfluid Phase Diagrams of Trapped Fermi Gases with Population Imbalance

Chih-Chun Chien, Qijin Chen, Yan He, and K. Levin

James Franck Institute and Department of Physics, University of Chicago, Chicago, Illinois 60637, USA

(Received 5 December 2006; published 13 March 2007)

We present phase diagrams for population-imbalanced, trapped Fermi superfluids near unitarity. In addition to providing quantitative values for the superfluid transition temperature, the pairing onset temperature, and the transition line (separating the Sarma and phase separation regimes), we study experimental signatures of these transitions based on density profiles and density differences at the center. Predictions on the BCS side of resonance show unexpected behavior, which should be searched for experimentally.

DOI: 10.1103/PhysRevLett.98.110404 PACS numbers: 03.75.Hh, 03.75.Ss, 74.20.−z

The study of ultracold trapped Fermi gases as they vary from BCS to Bose-Einstein condensation (BEC) is a rapidly exploding subject in condensed matter and atomic physics. In this Letter, we address the multiple superfluid and normal phases in these trapped gases, which are viewed as possible prototypes for quark and nuclear matter [1]. The various phases we contemplate become stable or unstable as one alters the populations [2–5] of the two spin species or changes the temperature T. There has been extensive theoretical literature on this subject which is almost exclusively confined to $T = 0$ [6–8]. Our emphasis here is on finite T effects [9,10], which are essential in order to address the actual experimental situation. Here we provide an understanding of existing data and present predictions for new experiments.

The fermionic superfluid ground state wave function in BCS-BEC crossover (with population imbalance) is almost universally assumed [6–8] to be of the BCS-Leggett form. The corresponding excitations consist of noncondensed pairs as well as gapped fermions in the interesting unitary regime. Noncondensed pairs (which are frequently omitted in the literature [11,12]) must be included for meaningful estimates of the ordering temperature T_c. As is consistent with experiments at unitarity [9], T_c is significantly lower than the pairing onset temperature T^* as a result of the opening of a pairing gap (or "pseudogap") above T_c. Without the contribution of noncondensed pairs, one often finds bimodal particle distributions for unpolarized gases, which are not observed experimentally [9,13]. Polarized gases, by contrast, exhibit [4] bimodality. Therefore, theories which ignore these pairs [11,12] may not be useful for establishing bimodal distributions specifically associated with population imbalance.

In the presence of population imbalance, one has to consider homogeneous phases (which we refer to as "Sarma") and Larkin-Ovchinnokov-Fulde-Ferrell (LOFF) phases [14] as well as phase separation [15]. In addition, the normal phase may appear as a highly correlated or paired state without phase coherence or as a simple (unpaired) Fermi gas phase. We begin with the (local) thermodynamical potential $\Omega_{\rm tot}$ (per unit volume) for the allowed states (excluding the more complicated LOFF phase, which appears to be of less interest near unitarity and at all but the lowest T [16]), in a harmonic trap potential $V_{\rm ext} = \frac{1}{2} m\bar{\omega}^2 r^2$, with mean angular frequency $\bar{\omega}$. For a normal or superfluid phase in which pairing correlations are present, $\Omega_{\rm tot}$ consists of contributions from gapped fermions (Ω_f) and noncondensed pairs or bosons (Ω_b):

$$\begin{aligned} \Omega_{\rm tot} &= \Omega_f + \Omega_b, \\ \Omega_f &= -\frac{\Delta^2}{U} + \sum_{\mathbf{k}} (\xi_k - E_k) - T \sum_{\mathbf{k},\sigma} \ln(1 + e^{-E_{k\sigma}/T}), \\ \Omega_b &= Z\mu_{\rm pair}\Delta_{\rm pg}^2 + T \sum_{\mathbf{q}} \ln(1 - e^{-\tilde{\Omega}_q/T}). \end{aligned} \quad (1)$$

Competing with this phase is the free Fermi gas phase, which has thermodynamical potential $\Omega_{\rm free} = -T\sum_{\mathbf{k},\sigma} \ln(1 + e^{-\xi_{k\sigma}/T})$. The (gapped) fermion and pair dispersions are given, respectively, by $E_{\mathbf{k}} = \sqrt{\xi_{\mathbf{k}}^2 + \Delta^2}$ for a contact (short-range) pairing interaction with strength U and $\tilde{\Omega}_q = q^2/2M^* - \mu_{\rm pair}$, where M^* and $\mu_{\rm pair}$ are the effective mass and chemical potential of the pairs, respectively. Both M^* and Z are obtainable from a microscopic T-matrix approach [10]. Here $E_{\mathbf{k}\sigma} = E_{\mathbf{k}} \mp h$ and $\xi_{\mathbf{k}\sigma} = \xi_{\mathbf{k}} \mp h$ for spins $\sigma = \uparrow$ and $\downarrow$, respectively, where $\xi_{\mathbf{k}} = k^2/2m - \mu$, $k_B = \hbar = 1$, with fermionic $\mu = (\mu_\uparrow + \mu_\downarrow)/2$ and $h = (\mu_\uparrow - \mu_\downarrow)/2$.

We distinguish the order parameter $\Delta_{\rm sc}$ from the total gap Δ. Noncondensed pairs contribute a pseudogap $\Delta_{\rm pg}$ to the total gap via $\Delta^2 = \Delta_{\rm sc}^2 + \Delta_{\rm pg}^2$. The form of Ω_b contains a free bosonlike contribution; the pair condensate does not contribute to Ω_b directly. Although it is not a necessary assumption, in order to simplify the formal description we assume that M^* depends only on T, as is reasonably consistent with our microscopic theory [10], and that $\mu_{\rm pair}$ depends only on Δ and T. Because pairs ultimately become diffusive by decay into the particle-particle continuum, in the summation over boson momentum $\mathbf{q}$, we will impose a cutoff $q < q_c$, where q_c is the minimum value of q which satisfies $E_k + \xi_{\mathbf{k}+\mathbf{q}} - \tilde{\Omega}_q = 0$ for at least one value of $\mathbf{k}$.

Note that Ω_f and Ω_b couple only via $\mu_{\rm pair}$. Above T_c, this leads to an extra contribution to the gap equation.

Our self-consistent equations, which have been presented in earlier papers [9,10], can be expressed equivalently as variational conditions on $\Omega_{\rm tot}$, for the total excitation gap Δ, the pseudogap $\Delta_{\rm pg}$, the fermion number density n, and the population imbalance δn, respectively:

$$\frac{\partial\Omega_{\rm tot}}{\partial\Delta}=0; \qquad \frac{\partial\Omega_{\rm tot}}{\partial\mu_{\rm pair}}=0;$$
$$-\frac{\partial\Omega_{\rm tot}}{\partial\mu}=n; \qquad -\frac{\partial\Omega_{\rm tot}}{\partial h}=\delta n.$$

Importantly, we have $\mu_{\rm pair}=0$ below T_c and $\Delta=\Delta_{\rm pg}$ above T_c. These equations reduce to the usual T-dependent BCS-like gap and number equations in the literature.

In a trap, T and h are independent of the radial position. The distribution of the local $\mu(\mathbf{r})$ is determined by the force balance equation $-\nabla\bar{p}=n\nabla V_{\rm ext}$, where $\bar{p}=-\Omega_{\rm tot}$ is the pressure. Using the number equation $n=-\partial\Omega_{\rm tot}/\partial\mu$, we obtain $\nabla\mu(\mathbf{r})=-\nabla V_{\rm ext}(\mathbf{r})$, or $\mu(\mathbf{r})=\mu_0-V_{\rm ext}(\mathbf{r})$, where $\mu_0\equiv\mu(0)$. Thus, force balance naturally leads to the usual local density approximation (LDA). To ensure meaningful comparisons between states under different conditions, we fix the total particle number $N=\int d^3rn(r)$ and the number difference δN. The Fermi energy $E_F=T_F\equiv k_F^2/2m$ is defined as that of a noninteracting gas with the same $N=N_\uparrow+N_\downarrow$ at polarization $p\equiv\delta N/N=0$. We assume $N_\uparrow>N_\downarrow$ so that $h>0$.

The physical state corresponds to the minimum of $\Omega_{\rm tot}$ and $\Omega_{\rm free}$. At a particular trap radius when (and if) these become equal, the system will have a first-order transition from a paired (but not necessarily superfluid) state to an unpaired Fermi gas phase. We assume an infinitely thin interface (i.e., domain wall) for this phase separation. There is as yet no complete microscopic theory for the interface energy, so we do not include it here. The philosophy behind our treatment of phase separation is very similar to that in previous $T=0$ papers [7,17] except that we include temperature effects (in a fashion consistent with the BCS-Leggett ground state). Across the interface, we require thermal, chemical, and mechanical equilibrium so that T, μ_σ, and $\bar{p}$ are continuous.

Figure 1 shows the phase diagram at unitarity for a polarized Fermi gas in a trap. Here $1/k_Fa=0$, where a is the s-wave scattering length between fermions. As in previous work [5,12,18], a tricritical point (TCP) exists. Phase separation (labeled PS) occupies the lower T portion of the phase diagram, where the gap Δ jumps abruptly to zero at some trap radius. At intermediate T, there is a (yellow-shaded) Sarma phase, where Δ vanishes continuously within the trap. Away from $p\equiv 0$, a minimum temperature is required [19] to arrive at the Sarma phase, due to the well-documented negative $T=0$ superfluid density. This Sarma state evolves into a (dotted) pseudogap (PG) phase as the superfluid core vanishes at higher T. An

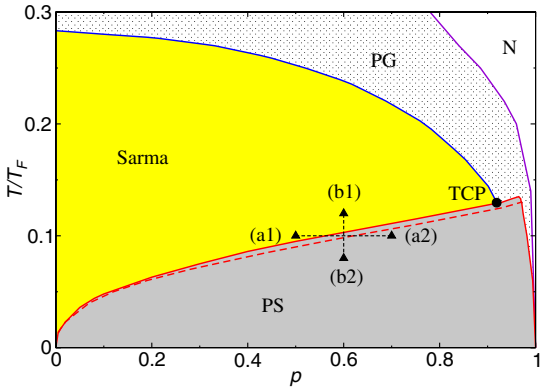

FIG. 1 (color online). Phase diagram of a population-imbalanced Fermi gas in a harmonic trap at unitarity. The solid lines separate different phases. Above the (red) dashed line but within the PS phase, the superfluid core does not touch the domain wall. Here "PG" indicates the pseudogapped normal phase. The black dot labeled "TCP" indicates the tricritical point. The four points indicated by the triangles labeled (a1)–(b2) correspond to the density profiles in Fig. 2.

(unpaired) normal (N) phase always exists at even higher T. In contrast with earlier work [11,12], here we include pair fluctuations or noncondensed pairs, which are essential in order to obtain quantitatively correct values for T_c as well as for the finite T particle density profiles [9,13]. Pairing fluctuations were partially included (through the number equation) in Ref. [18] based on the Nozières–Schmitt-Rink (NSR) scheme [20] but in the absence of a trap. We note that the finite T NSR treatment is not consistent with the standard ground state used here [6–8].

We stress that, with or without the trap, the PS phase is the ground state at unitarity for any p. Here we generalize phase separation to include either a superfluid or a correlated (paired) normal phase interfacing an uncorrelated normal gas. In the narrow regime above the (red) dashed line in Fig. 1, a superfluid core resides in the center, while a wall separates a correlated and an uncorrelated normal phase both outside the core.

In Fig. 2, we present four representative density profiles which show the behavior on different sides of the transition line between the PS and Sarma phases. The (a1)-(a2) pair have the same T but different p, while the (b1)-(b2) pair have the same p but different T. We have chosen these points some distance from the transition line in order to illustrate the differences. It should be noted, however, as points (a1) and (b1) (within the Sarma phase) move closer to the transition line, Δ drops rapidly (but not discontinuously), as a precursor to phase separation. The transition from the pure Sarma to the PS phase is, thus, a relatively smooth one. These LDA-based calculations should apply to situations where the trap geometry is reasonably isotropic, as, e.g., in the Massachusetts Institute of Technology (MIT) experiments [2,4], and where one might be able to ignore surface energy contributions. On the other hand, this behavior appears at odds with recent experi-

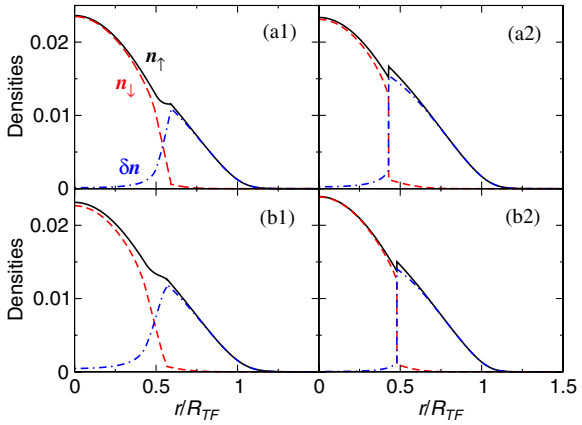

FIG. 2 (color online). Three-dimensional density profiles corresponding to the four points labeled in the phase diagram at unitarity shown in Fig. 1: (a1) $T = 0.1T_F$, $p = 0.5$; (a2) $T = 0.1T_F$, $p = 0.7$; (b1) $T = 0.12T_F$, $p = 0.6$; (b2) $T = 0.08T_F$, $p = 0.6$. The (black) solid, (red) dashed, and (blue) dotted-dashed lines correspond to $n_\uparrow$, $n_\downarrow$, and δn, respectively. Here $R_{\mathrm{TF}} = \sqrt{2E_F/m\bar{\omega}^2}$ is the Thomas-Fermi radius, and the units for density are k_F^{-3}.

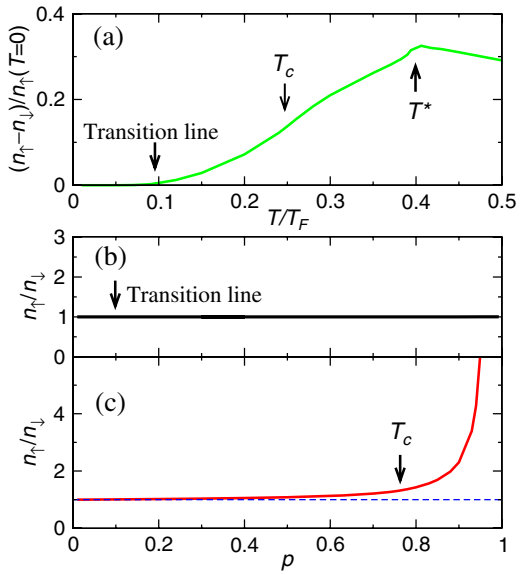

FIG. 3 (color online). Behavior at the trap center at unitarity: (a) $(n_\uparrow - n_\downarrow)/n_\uparrow(T = 0)$ as a function of T/T_F at fixed $p = 0.5$, and $n_\uparrow/n_\downarrow$ as a function of p at fixed (b) $T = 0.05T_F$ and (c) $T = 0.2T_F$. The (blue) dashed line in (c) indicates $n_\uparrow/n_\downarrow = 1$. The PS-Sarma transition line, T_c, and (pairing onset) T^* are indicated by arrows.

ments from Rice [3,5], which report pronounced changes in the aspect ratio of the profile as the transition line is crossed. These changes have been attributed to extreme trap anisotropy and associated interface energy effects [21].

In a different class of experiments, it was proposed that, by measuring densities at the trap center as one sweeps T or p, one can infer when the Sarma-PS transition line is crossed [22] as well as where superfluid transition [i.e., $T_c(p)$] occurs [5]. In Fig. 3(a), we plot $(n_\uparrow - n_\downarrow)/n_\uparrow(T = 0)$ at the trap center as a function of T at $p = 0.5$. This result is very similar to that of the MIT experiment [22]. When p is fixed at a relatively high value, the curve starts at 0 in the PS regime at low T and begins to increase with T when the PS-Sarma transition line is crossed. This behavior reflects that Sarma states can accommodate higher core polarizations than their PS counterparts.

The plots of $n_\uparrow/n_\downarrow$ at the trap center shown in Figs. 3(b) and 3(c) at fixed T while sweeping p are closely analogous to the results of the Rice experiment [5]. In Fig. 3(b), T is below the TCP and the curve is a horizontal line ($n_\uparrow/n_\downarrow = 1$), indicating that the core has equal population in both the Sarma state at low T and the PS phase at any (T, p). This figure also underlines the fact that PS states exist up to very high polarizations ($p > 0.99$). Finally, when T/T_F is higher than that of the TCP [Fig. 3(c)], the ratio increases rapidly after the superfluidity disappears, as appears to be observed experimentally [5]. Figure 3(c) reveals that when superfluidity is present, it resides in the trap center, expelling the excess fermions outside the core. If one performs the same experiment as in Fig. 3(a), but with much lower p (not shown), the crossing of the transition line will be barely observable, as is necessary in order to be consistent with Fig. 3(b). No matter how the Sarma-PS transition line is crossed, at low p (and thus low T), the ratio $n_\uparrow/n_\downarrow$ remains 1. Therefore, this class of experiments may not map out the transition curve for all p. Finally, Fig. 3(b) can be contrasted with the MIT experiments [2], where an upper critical polarization $p_c \approx 0.8$ for superfluidity is found. A measured condensate fraction of 55% at $p = 0$ suggests $T/T_c \gtrsim 0.6$ (at high p), which may not be inconsistent with p_c inferred from Fig. 1. A recent theoretical study [23] suggests that this reduced p_c may also be partly associated with a Hartree self-energy, not included in the BCS-like wave function discussed here.

Our theory can be generalized to address the whole of BEC-BCS crossover. As one passes from unitarity towards the BEC regime, we find that the fraction of the PS phase in the phase diagram decreases progressively, disappearing at $1/k_F a \approx 2.04$. For stronger couplings, the superfluid contribution to the phase diagram consists only of the Sarma phase, at all T. The same observation at $T = 0$ was first reported in Ref. [24]. This can also be inferred from the homogeneous phase diagram in Ref. [19], which shows that the Sarma state is stable at low T for any p providing $1/k_F a \gtrsim 2.3$.

In Fig. 4, we present a phase diagram similar to Fig. 1 but on the BCS side of resonance, where $1/k_F a = -0.5$. It differs significantly from the unitary case and is, in many ways, even richer. Importantly, at $T = 0$, the PS phase is no longer stable at very high p. We understand this by noting that, in the BCS regime, the pairing interaction is relatively weak and the gap Δ small. At sufficiently high p, we have $h > \Delta(r = 0)$, so that an unpolarized BCS superfluid core can no longer be sustained.

Equally important is the fact that, in this BCS case, the Sarma and PS phases do not connect and an intermediate

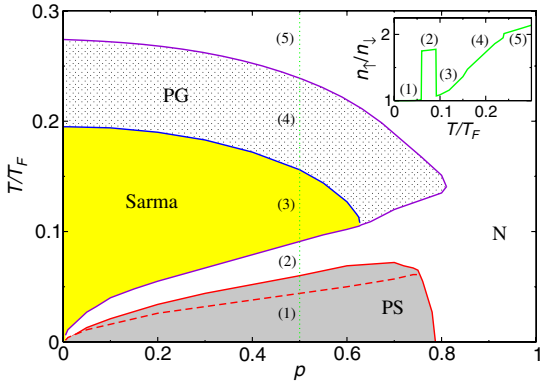

FIG. 4 (color online). Phase diagram of a polarized Fermi gas, as in Fig. 1 except that $1/k_F a = -0.5$. Here the Sarma and PS phases are separated by an intermediate normal regime. The (green) dotted line indicates a sweep of T at $p = 0.5$, with five possible structures labeled (1) PS, (2) N, (3) Sarma, (4) PG, and (5) N. Shown in the inset is $n_\uparrow/n_\downarrow$ at the trap center vs T/T_F.

phase appears in between. As a consequence, the boundaries of the Sarma, PS, and (pseudogapped or unpaired) normal phases do not meet except possibly at $p = T = 0$. We presume that this intermediate phase is a normal Fermi gas (N). To understand its appearance, we note that as the BCS regime is approached, (i) phase separation becomes problematic because finite temperature (which enters via T/Δ) has a stronger effect, allowing the polarization to penetrate into the center of the core and thereby making PS more difficult. (ii) In addition, the intermediate T Sarma phase becomes more fragile as the pairing is weakened. As a result, the Sarma and PS states retreat from each other as seen in Fig. 4. We cannot rule out LOFF-like states as an alternative candidate in place of N. However, we have found [16] that these phases, in general, have very low T_c and should not persist at these higher temperatures. In the inset in Fig. 4, we plot $n_\uparrow/n_\downarrow$ at the trap center as a function of T/T_F. The N state between the PS and Sarma phases would be manifested by sudden jumps at the PS-N and N-Sarma boundaries. This prediction can be used to test the existence of the intermediate N state in the phase diagram. Finally, like its counterpart in Fig. 1, the sliver in the PS phase above the (red) dashed line in Fig. 4 corresponds to phase separation between a *correlated* normal and a free Fermi gas.

We end with another prediction concerning how the ''mixed normal'' region of the trap, emphasized experimentally in Ref. [4], evolves with T. As noted in earlier work [25], within the Sarma phase, this mixed normal state consists of highly correlated noncondensed pairs which necessarily become less significant as T decreases. However, with decreasing T, as seen from Figs. 1 and 4, the Sarma phase gives way to stable phase separation. Everywhere in the PS phase, there is a mixed normal region in the gas outside the domain wall, with no pairing correlations, as was found at strictly $T = 0$ [7,8]. Thus, a change should occur from a highly correlated to an uncorrelated mixed normal region at large radii as T is progressively decreased. Further experiments should help to address these predictions.

This work was supported by Grants No. NSF PHY-0555325 and No. NSF-MRSEC DMR-0213745; we thank R. G. Hulet, M. W. Zwierlein, W. Ketterle, C. Chin, and Y. Shin for useful conversations.

[1] M. M. Forbes, E. Gubankova, W. V. Liu, and F. Wilczek, Phys. Rev. Lett. **94**, 017001 (2005).
[2] M. W. Zwierlein, A. Schirotzek, C. H. Schunck, and W. Ketterle, Science **311**, 492 (2006).
[3] G. B. Partridge, W. Li, R. I. Kamar, Y. A. Liao, and R. G. Hulet, Science **311**, 503 (2006).
[4] M. W. Zwierlein, C. H. Schunck, A. Schirotzek, and W. Ketterle, Nature (London) **442**, 54 (2006).
[5] G. B. Partridge, W. Li, Y. A. Liao, R. G. Hulet, M. Haque, and H. T. C. Stoof, Phys. Rev. Lett. **97**, 190407 (2006).
[6] D. E. Sheehy and L. Radzihovsky, Phys. Rev. Lett. **96**, 060401 (2006).
[7] T. N. De Silva and E. J. Mueller, Phys. Rev. A **73**, 051602(R) (2006).
[8] M. Haque and H. T. C. Stoof, Phys. Rev. A **74**, 011602(R) (2006).
[9] Q. J. Chen, J. Stajic, S. N. Tan, and K. Levin, Phys. Rep. **412**, 1 (2005); K. Levin and Q. J. Chen, cond-mat/0611104.
[10] Q. J. Chen, H. Yan, C.-C. Chien, and K. Levin, Phys. Rev. B **75**, 014521 (2007).
[11] K. Machida, T. Mizushima, and M. Ichioka, Phys. Rev. Lett. **97**, 120407 (2006).
[12] K. B. Gubbels, M. W. J. Romans, and H. T. C. Stoof, Phys. Rev. Lett. **97**, 210402 (2006).
[13] J. Stajic, Q. J. Chen, and K. Levin, Phys. Rev. Lett. **94**, 060401 (2005).
[14] P. Fulde and R. A. Ferrell, Phys. Rev. **135**, A550 (1964); A. I. Larkin and Y. N. Ovchinnikov, Zh. Eksp. Teor. Fiz. **47**, 1136 (1964) [Sov. Phys. JETP **20**, 762 (1965)].
[15] P. F. Bedaque, H. Caldas, and G. Rupak, Phys. Rev. Lett. **91**, 247002 (2003); H. Caldas, Phys. Rev. A **69**, 063602 (2004).
[16] Y. He, C.-C. Chien, Q. J. Chen, and K. Levin, Phys. Rev. A **75**, 021602(R) (2007).
[17] F. Chevy, Phys. Rev. Lett. **96**, 130401 (2006).
[18] M. M. Parish, F. M. Marchetti, A. Lamacraft, and B. D. Simons, Nature Phys. **3**, 124 (2007).
[19] C.-C. Chien, Q. J. Chen, Y. He, and K. Levin, Phys. Rev. Lett. **97**, 090402 (2006).
[20] P. Nozières and S. Schmitt-Rink, J. Low Temp. Phys. **59**, 195 (1985).
[21] T. N. De Silva and E. J. Mueller, Phys. Rev. Lett. **97**, 070402 (2006).
[22] Y. Shin, M. W. Zwierlein, C. H. Schunck, A. Schirotzek, and W. Ketterle, Phys. Rev. Lett. **97**, 030401 (2006).
[23] C. Lobo, A. Recati, S. Giorgini, and S. Stringari, Phys. Rev. Lett. **97**, 200403 (2006).
[24] P. Pieri and G. C. Strinati, Phys. Rev. Lett. **96**, 150404 (2006).
[25] C.-C. Chien, Q. J. Chen, Y. He, and K. Levin, Phys. Rev. A **74**, 021602(R) (2006).